

# The on-ground calibration of the Ozone Monitoring Instrument from a scientific point of view

Ruud Dirksen<sup>\*ab</sup>, Marcel Dobber<sup>a</sup>, Pieter Levelt<sup>a</sup>, Gijsbertus van den Oord<sup>a</sup>, Glen Jaross<sup>c</sup>, Matt Kowalewski<sup>c</sup>, George H. Mount<sup>d</sup>, Don Heath<sup>e</sup>, Ernest Hilsenrath<sup>f</sup>, Johan de Vries<sup>g</sup>

<sup>a</sup>Royal Netherlands Meteorological Institute, PO Box 201, 3730 AE De Bilt, NL;

<sup>b</sup>Space Research Organisation Netherlands, Sorbonnelaan 2, 3584 CA Utrecht, NL;

<sup>c</sup>Science systems & Applications Inc, GSFC-Code 916, Greenbelt, MD USA 20771;

<sup>d</sup>Dept. of Civil and Env. Engineering, Washington State University, Pullman, WA USA 99164;

<sup>e</sup>Research Support Instruments Inc, 5735 Arapahoe Ave., suite 2A, Boulder, CO USA 80303;

<sup>f</sup>Atmospheric Chemistry and Dynamics branch, GSFC-code 916, Greenbelt, MD USA 20771;

<sup>g</sup>Dutch Space BV, Postbus 32070, 2303 DB Leiden, NL

## ABSTRACT

The Ozone Monitoring Instrument is an UV-Visible imaging spectrograph using two-dimensional CCD detectors to register both the spectrum and the swath perpendicular to the flight direction. This allows having a wide swath (114 degrees) combined with a small ground pixel (nominally 13 x 24 km<sup>2</sup>). The instrument is planned for launch on NASA's EOS-AURA satellite in January 2004. The on-ground calibration measurement campaign of the instrument was performed May-October 2002, data is still being analyzed to produce the calibration key data set. The paper highlights selected topics from the calibration campaign, the radiometric calibration, spectral calibration including a new method to accurately calibrate the spectral slitfunction and results from the zenith sky measurements and gas cell measurements that were performed with the instrument.

**Keywords:** calibration, remote sensing, UV-Visible, imaging spectrograph, trace gases

## 1. INTRODUCTION

The primary objective of OMI-EOS is to obtain global measurements of a number of trace gases in both the troposphere and stratosphere. These measurements are meant to address science questions on the recovery of the ozone layer, the depletion of ozone at the poles, tropospheric pollution and climate change.

The constituents are retrieved from nadir observations of backscattered light from the Sun on the Earth's atmosphere in the UV-Visible wavelength range (270 to 500nm). Within this range, the spectral properties are such that it is possible to use both DOAS and TOMS-type of algorithms for column retrievals of the various atmospheric constituents. The ozone profile is obtained from the rapid increase of the absorption cross-section towards shorter wavelength in the UV. The retrieval methods used for instruments like GOME, SCIAMACHY, TOMS and SBUV can be applied to OMI spectra.

In order to meet the science objectives measurements are needed that combine both very good spatial resolution and daily global coverage. The high spatial resolution is required to optimize the chance of observing cloud-free ground pixels. This is important for obtaining the best tropospheric trace gas amounts and to enable OMI-EOS to monitor tropospheric pollution phenomena, like biomass burning and industrial pollution, on a regional scale. Recording tropospheric pollution is essential for studying human impact on the Earth's atmosphere and climate.

OMI-EOS will deliver the spectral radiances and irradiances from 270 to 500 nm and these are used to retrieve the following primary data products: ozone total column, ozone vertical profile, UV-B flux, NO<sub>2</sub> total column, aerosol optical thickness, cloud effective cover and cloud top pressure. Next to these are the following additional products: SO<sub>2</sub>, BrO, HCHO and OCIO.

The cloud top pressure is obtained from the Ring effect due to Raman inelastic scattering at 390-400 nm and from O<sub>2</sub>-O<sub>2</sub> absorption. The cloud cover and aerosol optical thickness are obtained from the broader wavelength dependency of the

sunlight backscattered from the Earth's atmosphere. By employing a polarization scrambler the instrument is made insensitive to the polarization of the incoming radiances.

OMI has been developed by Dutch and Finnish industry in close collaboration with the climate research and meteorological community and under contract with the Netherlands Agency for Aerospace Programmes (NIVR) and the Finnish Meteorological Institute (FMI). The Royal Netherlands Meteorological Institute (KNMI) is the PI institute for the OMI instrument. The international OMI science team has approximately 40 members. The instrument will be launched on NASA's EOS-AURA satellite, in January 2004 that will fly in a polar sun-synchronous orbit at approximately 700km altitude and its operational temperature is  $-8.5$  degrees centigrade.

The integration of the OMI proto-flight model (PFM) was completed in 2001 and was instantly followed by an extensive performance test program, spanning multiple months, which showed the OMI instrument to meet its design requirements. The on-ground calibration measurement campaign lasted from May till October 2002 and comprised of measurements performed in ambient and in flight representative thermal vacuum conditions. After conclusion of the calibration period the OMI instrument was shipped for integration on the spacecraft. Tests on the integrated system are ongoing.

For remote sensing instruments like OMI a good quality of the on-ground calibration delivering reliable calibration key data is essential to meet the required accuracies of the scientific data products, especially when the data is to be compared to and to become part of long-term ozone trend recordings. The on-ground calibration of the OMI instrument was performed by and under responsibility of industry, with the scientific users having an advisory role.

The preliminary results of the on-ground calibration, analysis of the calibration key data is still ongoing, seen from the perspective of the scientific user is the focus of this paper.

## 2. OMI INSTRUMENT DESCRIPTION

The OMI instrument is a compact nadir viewing UV-VIS imaging spectrograph with two spectral channels each having a two-dimensional frame transfer CCD. The large field-of-view (FOV)( $114^\circ$ ) perpendicular to the flight direction yields a 2600km wide swath that is large enough to achieve global daily coverage of the Earth's atmosphere at the equator. The swath is sampled by 60 pixels; the size of a pixel projected on the Earth's surface is  $13 \times 24 \text{ km}^2$  (flight direction x swath direction) in the nadir direction. This small ground pixel size increases the chance of observing cloud-free pixels. By employing a 2D CCD the spectrum of every ground pixel is recorded simultaneously preventing spatial aliasing resulting from using a scan mirror. In one dimension of the CCD the spectrum is registered (also called the spectral direction) while the FOV is recorded in the other dimension.

A layout of the OMI optical bench depicting the telescope and the UV spectral channel is presented in figure 1; the large swath is out of the plane of the paper. The telescope consists of a primary mirror, a polarization scrambler and a secondary mirror, focusing the incident radiance on the spectrograph slit. Irradiances enter the instrument through the solar port, which has a 10% transmission solar mesh, and illuminate a reflection diffuser. A folding mirror couples the diffuser signal into the main optical path just before the polarization scrambler. An on-board White Light Source (WLS) is coupled in through a transmission diffuser and the same folding mirror. For on-ground calibration purposes this optical path was also used by mounting external stimuli on a calibration port close to the WLS. The beam coming of either of the on-board diffusers illuminates the full length of the spectrograph slit and thereby all viewing directions (CCD rows) within the field-of-view. After the slit, in the spectrograph the beam is split into two channels: the UV (270-380 nm) and the Visible (350-500 nm). The UV channel is separated into two sub-channels: UV1 (270-310 nm) and UV2 (300-380 nm) by the two-part mirror labeled 104. This decreases the straylight at smaller wavelengths, furthermore the UV1 channel is scaled down by a factor two in both dimensions, meaning that both the spectral and spatial sampling distances are 2 times larger as compared to the UV2 sub-channel. This is to improve the ratio between useful and dark signals in the UV1. The spectral sampling distances are 0.32nm, 0.15nm and 0.21nm for UV1, UV2 and VIS respectively. The ratio between the spectral resolution and the sampling distance is about 3 in UV2 and VIS to avoid any difficulties caused by aliasing in the process of trace gas retrieval.

The net integration time of 2 seconds, consisting of co-added 0.4s individual exposures, sets the spatial sampling in the flight direction to 13km. The CCD detector has a frame transfer layout to allow simultaneous exposure and readout of the previous exposure, avoiding data loss during readout. In the nominal operational mode (global mode) 8 CCD rows are added (binned) during the readout, so spectra from neighboring viewing directions are summed. This decreases the

contribution of the readout noise and the internal data rate, and it increases the signal to noise. This sets the ground pixel size in the swath direction to 24 km.

The spatial and spectral properties of the OMI instrument are summarized in the following table.

|      | Wavelength range (nm) | Sampling (nm/pixel) | Resolution (nm) | Pixel size (binning 8) |
|------|-----------------------|---------------------|-----------------|------------------------|
| UVI  | 270-310               | 0.32                | 0.65            | 13x48 km <sup>2</sup>  |
| UVII | 305-375               | 0.15                | 0.45            | 13x24 km <sup>2</sup>  |
| VIS  | 350-500               | 0.21                | 0.65            | 13x24 km <sup>2</sup>  |

Table 1: spectral and spatial properties for the channels of the OMI instrument.

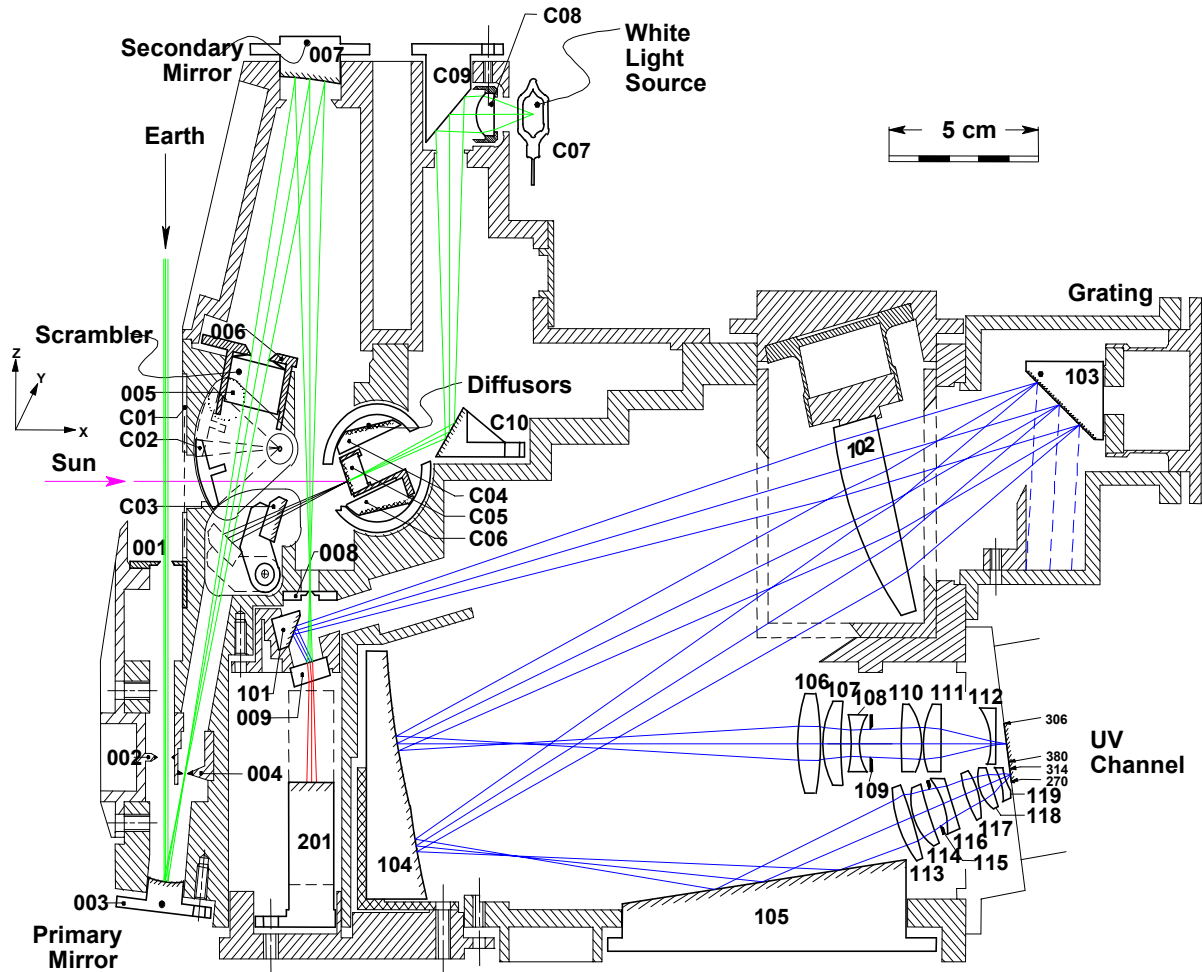


Figure 1: Layout of the optical bench of the OMI instrument. Telescope + UV spectral channel.

For in-flight calibration the OMI instrument is equipped with the following possibilities:

- A set of three reflective diffusers for absolute radiometric calibration by daily measurement of the Sun. Two of the three diffusers are conventional grinded aluminum diffusers, one to be used on a weekly basis the other to be used monthly to monitor the degradation of the first diffuser. The degradation is expected to a function of the integrated sun light exposure time. The third diffuser is a double grinded quartz volume diffuser that is to be used on a daily basis. This volume diffuser was implemented because in the SCIAMACHY program it was found that grinded aluminum diffusers exhibit wavelength dependent structures that affect the accuracy of the

radiometric calibration and that interfere with the DOAS retrieval of data products. Because of its smooth surface the spectral structures introduced by the volume diffuser are much smaller. The diffusers are well protected from contamination and irradiance while not in use.

- The WLS provides relative radiometric calibration and information about the degradation of the detector (bad/dead pixels).
- Two LEDs per (sub)channel mounted in the proximity of the detector are also used to trace bad/dead pixels.
- At the eclipse side of the orbit the dark signal is calibrated by performing both long exposure time dark measurements and dark signal measurements with instrument settings identical to radiance measurements at the dayside of the orbit.
- Spectral calibration is being performed using Fraunhofer lines in solar and nadir spectra. The OMI spectral slitfunction is known with high accuracy from the on-ground calibration; this precise knowledge of the slitfunction allows a wavelength calibration between a high-resolution solar spectrum and the observed features.

### 3. RADIOMETRIC CALIBRATION

Past experience with other satellite instruments (GOME, SCIAMACHY, TOMS (S)SBUV) has shown that it is extremely important to obtain and measure any type of calibration parameter, but the radiometric calibration parameters in particular, under flight-representative thermal-vacuum pressure and temperature conditions, because outgassing of coated optical components and alignment changes over a 30 K temperature range will introduce considerable changes that can not be predicated in advance. For the on-ground calibration of the OMI instrument radiance earth mode and the irradiance sun mode are radiometrically calibrated in absolute sense under flight representative thermal vacuum pressure and temperature conditions (-8.5°C) for one viewing geometry. The determination of the viewing angle dependency of the absolute radiance and irradiance calibration parameters relies on ambient measurement data. The same approach was followed for the calibration of the OMI instrument Bi-directional Spectral Distribution Function (BSDF) which is the key parameter to calibrate the earth reflectance (the Earth radiance measurement divided by the solar irradiance measurement, the base input for the data product retrieval algorithms)

As is seen in the optical layout presented in figure 1 the optical path for the radiance and the irradiance mode is identical save the primary telescope mirror that is unique for the radiance path and the solar mesh, the on-board diffuser and the folding mirror, that are unique to the irradiance path. The other optical components in the OMI instrument are common for the (ir)radiance path and therefore are assumed to cancel in the ratio irradiance/radiance measurement, which basically constitutes the instrument BSDF. Consequently the instrument BSDF includes the efficiency of the on-board diffuser, the solar mesh, and the primary and the folding mirror, of which the spectral dependency of the reflectivity of the on-board diffuser is assumed to be dominant. As was mentioned in the previous section, in the SCIAMACHY project it was found that the aluminum on-board diffusers introduce spectral features in the irradiance signal. These features result from white light interference caused by the diffuser surface and may interfere with trace gas absorption structures in the earth reflectance spectrum and thereby hinder the retrieval of the column densities of these gases. To remedy this a new type of volume diffuser was developed that has much better spectral feature behavior. This new diffuser is a doubly grinded quartz plate with one reflective, aluminum coated, surface. Being scattered by three surfaces effectively reduces interference effects. The absolute radiometric calibration, the BSDF calibration and the diffuser spectral features each are treated in a separate subsection.

#### 3.1 Absolute radiometric calibration

The absolute radiance calibration of the OMI instrument was performed employing a FEL lamp, a NIST traceable radiometric standard, and a 30x30cm<sup>2</sup> labsphere spectralon diffuser panel. The absolute irradiance calibration was derived by combining the absolute radiance calibration and the OMI instrument BSDF, that is discussed in the next section. The FEL lamp was used in a NIST prescribed setup for absolute radiance calibration: the FEL lamp illuminating the spectralon diffuser panel perpendicularly from a 50.0 cm distance. The OMI instrument was residing in a thermal vacuum chamber at stable flight representative vacuum pressure and temperature conditions. Appropriate measures were taken to prevent stray light reflections from the interior walls of the vacuum chamber. A 40-degree viewing angle on the diffuser panel was employed; the BRDF of the spectralon diffuser was calibrated for this viewing geometry by the TNO institute of applied physics (TNO-TPD) in the Netherlands and at the NASA-GSFC radiometric calibration facilities. The measurements were repeated with three different NIST calibrated FEL lamps. In the employed setup for absolute radiance calibration only a small part (~4 degrees) of the 114 degree large field-of-view of the OMI instrument was illuminated and because it was not possible to rotate the OMI instrument in the thermal vacuum chamber the absolute

radiance calibration at flight representative thermal vacuum temperature and pressure conditions is only available for nadir zero viewing angle. The viewing angle dependence of the absolute radiance sensitivity of the OMI instrument for off nadir viewing angles is derived from the viewing angle dependence of the radiance sensitivity measured in ambient. The absolute radiance sensitivity of the OMI instrument at flight representative thermal vacuum conditions for nadir 0 viewing angle is shown in figure 2. The enhanced sensitivity of the UV1 spectral channel that is achieved by scaling down the channel both in the spectral and in the spatial dimension is clearly visible in the plot.

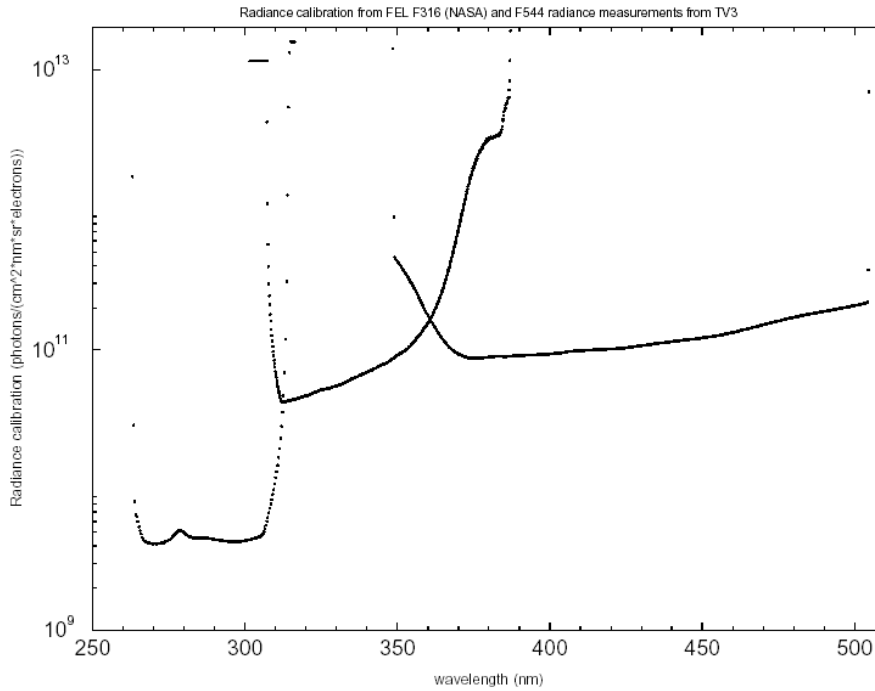


Figure 2: The absolute radiance calibration of the OMI instrument for nadir zero viewing direction, measured at flight representative thermal vacuum pressure and temperature environmental conditions. The enhanced sensitivity in the UV1 spectral channel results from scaling down the channel by a factor two in both the spectral and the spatial dimension.

### 3.2 BSDF calibration

The BSDF of the OMI instrument was calibrated using a specially designed optical stimulus having a divergence of 0.5 degree, similar to the sun. The light source of the stimulus is a xenon plasma source, ensuring long-term stability during the radiance and irradiance measurements, which is preferable to using a FEL lamp which has a limited number of burning hours.

During the BSDF measurements the instrument was at stable flight representative thermal vacuum conditions. For deriving the absolute value of the OMI instrument BSDF the thermal vacuum measurements for nadir 0 degree viewing direction are used. The viewing angle dependency of the OMI instrument BSDF is inferred from ambient measurements as a consequence of the impossibility to freely rotate the OMI instrument in the thermal vacuum facility. The viewing angle dependency of the OMI instrument BSDF obtained from the ambient measurements was verified with one off-nadir measurement (+50 degree viewing direction) at flight representative thermal vacuum conditions, showing reasonable agreement between the viewing angle dependency of the OMI instrument BSDF at ambient and at thermal vacuum environmental conditions. The OMI instrument BSDF for nadir 0 degree measured at flight representative thermal vacuum conditions is presented in figure 3 for all three on-board diffusers. The BSDF curve for the quartz volume diffuser is approximately a factor two lower than the BSDF curves for the two aluminum diffusers. This results from the lower reflectivity of the quartz volume diffuser. There is a 15%, wavelength dependent, difference between both aluminum diffusers.

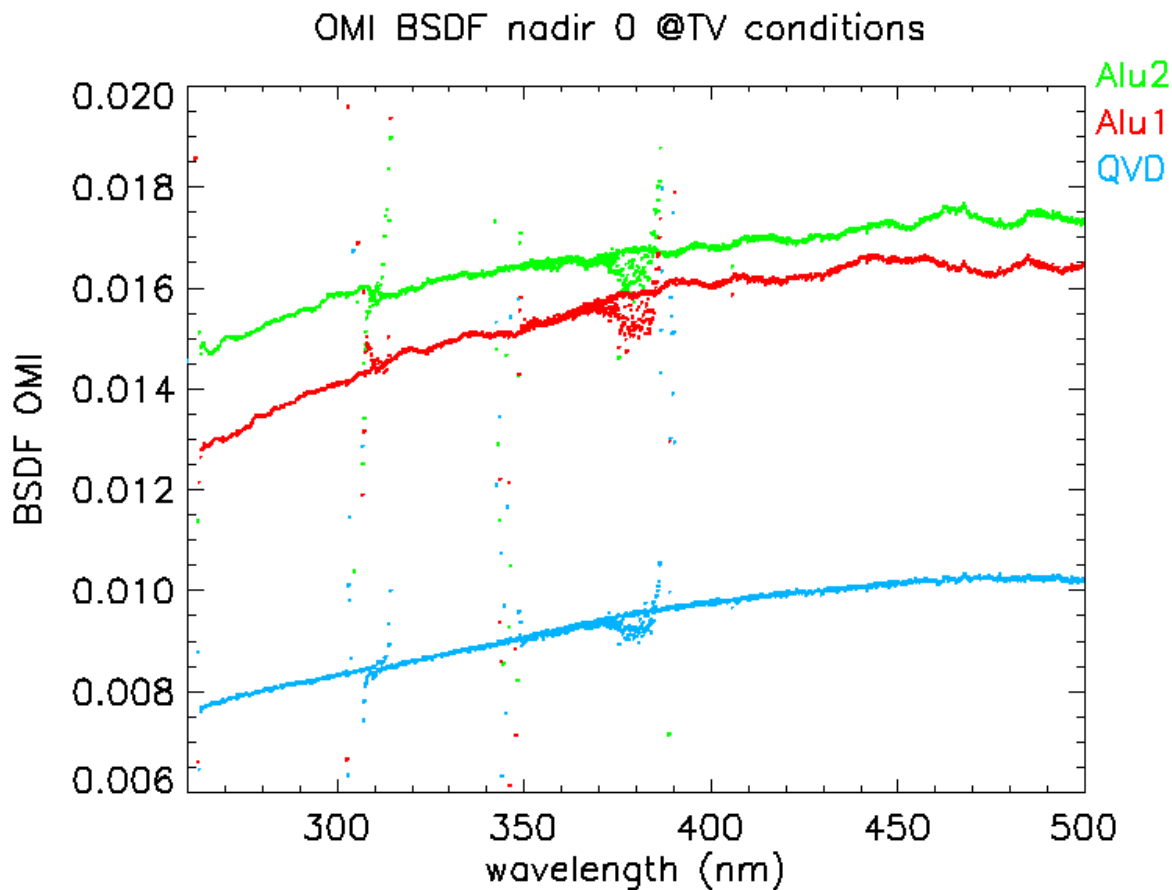


Figure 3: OMI instrument BSRF for nadir 0 degree viewing angles measured at thermal vacuum environmental conditions for all three on-board reflection diffusers.

### 3.3 Diffuser features

It was found in the SCIAMACHY project that aluminum reflection diffusers introduce spectral structures in the irradiance signal and consequently in the earth reflectance spectrum. These spectral features result from white light interference effects from the diffuser surface (resulting in a speckle pattern). The BSRF curves for the aluminum on-board diffusers presented in figure 3 clearly exhibit diffuser spectral features. When the period of these spectral features is comparable to trace gas absorption features they may interfere with DOAS-based retrieval of trace gases affecting the accuracy of the retrieved column densities. To remedy this the above-mentioned quartz volume diffuser, that because of its smooth surface exhibits much smaller spectral features, was developed and integrated in the instrument. The diffuser spectral features become clearly visible in the ratio of spectra taken at different illumination (azimuth and/or elevation) angles, and their size and behavior –rapid or slow variations with changing azimuth/elevation angle- can be studied this way. However the features in the ratioed irradiance measurements are not identical to the features as they show up in the earth reflectance spectrum. A limited measurement program was performed in ambient environmental conditions to assess the behavior of the spectral features at a rather coarse grid. Figure 4 shows the ratio of a single elevation measurement over the average of all elevation angles in the range  $-3.0, +3.0$  degrees for the quartz volume diffuser (left) and for the aluminum diffuser (right) for 310-500nm wavelength range. The size of the spectral features for the aluminum diffuser is 5-10% peak-peak whereas the feature size for the quartz volume diffuser evidently is much smaller. A 5% feature size would be disastrous for the retrieval of DOAS based data products as the size of absorption features of trace gases typically measure  $10^{-3}$ - $10^{-2}$ . Apart from affecting the DOAS retrieval the spectral features also influence the accuracy of the level 1 irradiance product. For a full characterization and calibration of the diffuser spectral features we have to rely on in-flight irradiance measurements and cross-calibrate the aluminum diffusers to the quartz volume diffuser for the full azimuth and elevation illumination angle range.

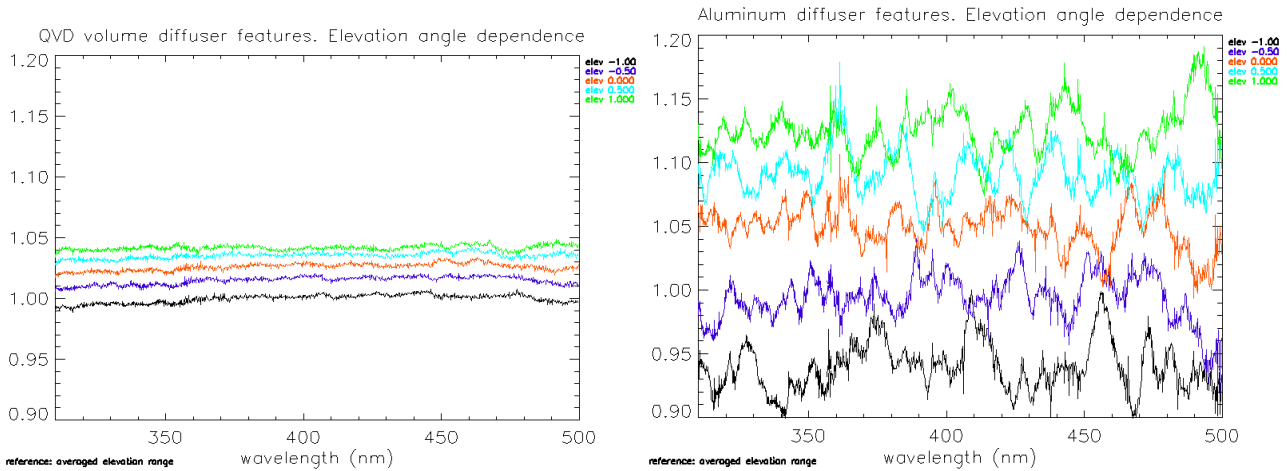


Figure 4: Ratio of single elevation angle measurement over the average of all elevation angles in the range [-3.0,+3.0] degrees for the quartz volume diffuser (left) and the aluminum diffuser (right) for the 310-500nm-wavelength range.

Beside spectral features the aluminum diffusers also exhibit spectrally independent features, with a size in the order of several percent, that manifest themselves in the spatial (row) direction of the irradiance illumination profile. These high frequent features are caused by randomly distributed specularly reflective spots on the grinded surface of the aluminum diffuser. The pattern of these wavelength independent features behaves erratic with illumination angle and their occurrence directly affects the viewing angle dependency of the OMI instrument BSDF. One of the reasons for the diffuser features to show up so profoundly is that a CCD detector pixel only samples a small area of the on-board diffuser, a consequence of the on-board diffusers being placed in the focus of the telescope, rendering the signal in the pixel sensitive to local wavelength (in)dependent variations of diffuser reflectivity rather than averaging them out as would be the case when a detector pixel sample the full area of the on-board diffuser.

#### 4. SPECTRAL CALIBRATION

The calibration of the spectral properties of the OMI instrument comprises two aspects: the spectral assignment and the shape of the spectral response function (slitfunction) of each detector pixel. Both calibration parameters were measured with the OMI instrument at flight-representative thermal vacuum pressure and temperature environmental conditions. The spectral resolution, or slitfunction, determines how spectral structures in the input (ir)radiance are smeared and recorded by the OMI instrument. This is of great importance for DOAS based retrieval of data products where the structures in the observed Earth reflectance spectrum are fitted by an accurate spectrum of the trace gas of interest smeared to OMI resolution in order to retrieve its slant column density. The exact shape of trace gas absorption spectrum at OMI resolution can be obtained either by measuring it directly in a laboratory setup using a gas cell, or by convolving a high-resolution literature absorption cross section spectrum with the accurately measured slitfunction. Early in the OMI project the choice was made to invest in an accurate calibration of the shape of the slitfunction rather than performing gas cell measurements at various pressures and temperatures. For the purpose of accurately measuring the slitfunction shape a dedicated optical stimulus was designed that utilizes an Echelle grating to produce an output beam containing ~50 tunable, well separated, narrow spectral peaks (diffraction orders) in the OMI wavelength range. By turning the Echelle grating the peak positions in the stimulus output beam move in wavelength space. The response of a detector pixel to a passing Echelle peak constitutes the spectral slitfunction of that pixel. By employing this method the shape of the spectral slitfunction is measured with better sampling, and at higher accuracy, than is obtained using a spectral line source, in which case the accuracy is limited by the sampling of the spectral resolution by the detector. As listed in table 1 the ratio spectral resolution/sampling of the OMI instrument typically is 3, whereas in the dedicated slitfunction measurements a ten times better sampling of the spectral resolution is achieved. The light beam of the stimulus was coupled into the OMI instrument using the above mentioned calibration port, doing so the full length of the spectrograph slit and thereby all CCD-rows (viewing angles) were illuminated enabling the slitfunction profile of all CCD pixels to be measured in a single measurement run. During the PFM performance test period slitfunction measurements were performed illuminating the instrument through the nadir port, the sun port and the calibration port and it was verified that

the slitfunction measured via either of these illumination ports is identical. Figure 5 shows in the upper plot the sampling of the spectral slitfunction when recording the response to a spectral line source while the lower plot shows the improved sampling of the slitfunction measured using the dedicated optical stimulus. The solid line is a functional fit through the data points of the lower plot. The fit result is co-plotted in the upper panel. For the UV1 spectral channel a regular Gaussian line shape was fitted, for the UV2 and VIS spectral channels a modified, broadened Gaussian profile was used. The functional describing the broadened Gaussian profile is given in the following equation:

$$A_0 e^{-\left(\frac{x-x_0}{w_0}\right)^2} + A_1 e^{-\left(\frac{x-x_1}{w_1}\right)^4} \quad (1)$$

with  $A_0$ ,  $A_1$ ,  $x_0$ ,  $x_1$ ,  $w_0$ ,  $w_1$  being fitting parameters.

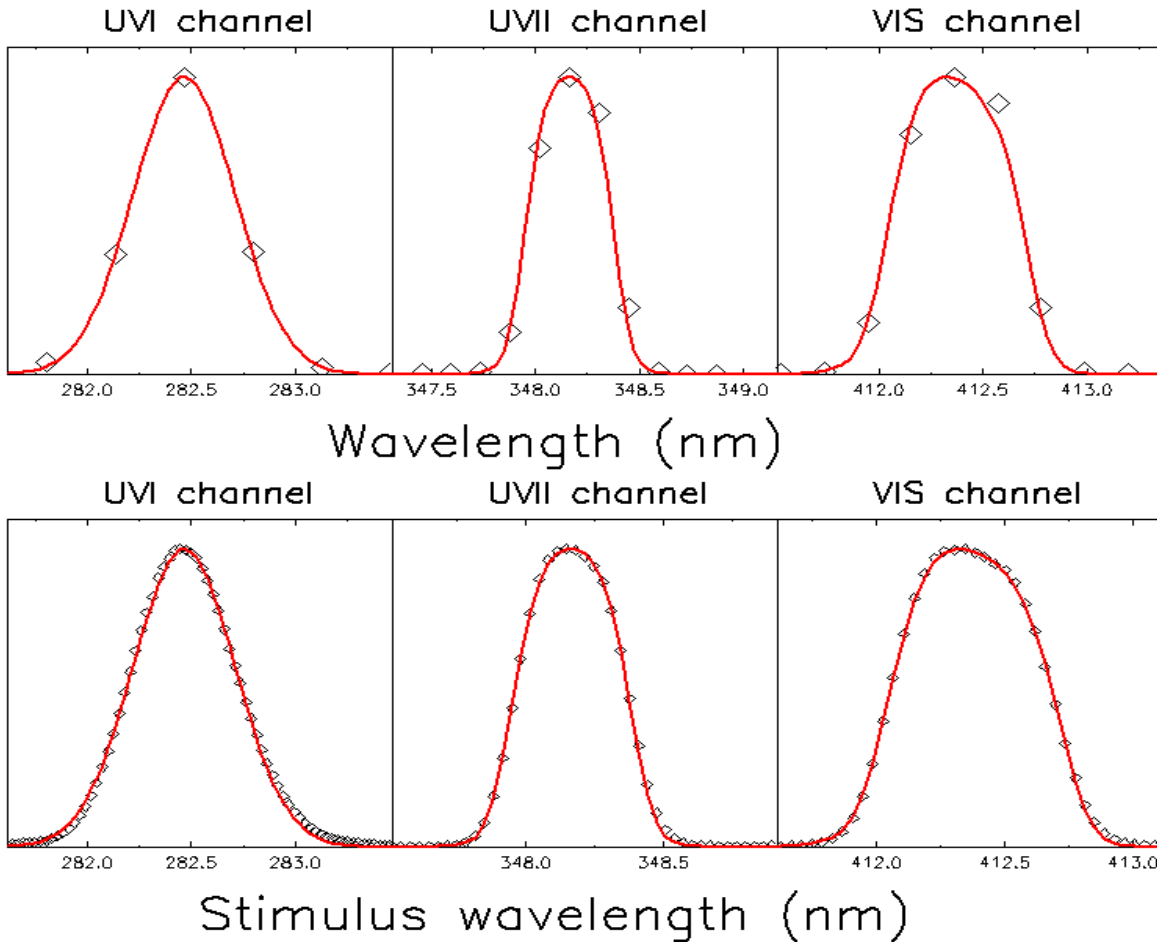


Figure 5: The OMI spectral slitfunction profile for each spectral channel. The upper panel presents the OMI response to a spectral line, the limited sampling of OMI's spectral resolution is clearly visible. The lower panel presents the OMI slitfunction calibrated with the dedicated optical stimulus; ten times better sampling is achieved with this stimulus. The solid line is a functional fit through the data, a Gaussian profile in UV1, a modified (broadened) Gaussian profile in UV2 and VIS. The fit result of the lower panel is co-plotted in the upper panel.

In the next section, presenting the results of gas cell and zenith sky measurements performed with the OMI instrument, a  $\text{NO}_2$  gas cell measurement is compared to a high-resolution literature  $\text{NO}_2$  cross-section spectrum convolved with the calibrated OMI slitfunction, validating the approach followed in the OMI project to accurately measure the spectral slitfunction. Although it is part of the calibration keydata base, the slitfunction itself won't be used directly in processing the level 0 data. Instead a high-resolution solar spectrum convolved with the slitfunction will be used for in-orbit

wavelength calibration. As mentioned earlier in this section the slitfunction will be part of the level 2 data processing in the form of a convolved trace gas absorption spectrum.

The calibration of the spectral assignment was performed using a hollow cathode PtCrNe spectral line source. As this line source lacks sufficiently strong lines in the high end of the OMI wavelength range, these measurements were combined with the slitfunction measurement data to derive a sufficiently accurate wavelength calibration, yielding an on-ground wavelength calibration accuracy of 1/10 pixel ( $\sim 0.01\text{nm}$ ). This is sufficiently accurate for the analysis of the other on-ground calibration measurement data. The required accuracy for the in-flight wavelength calibration, 1/100 pixel, will be met using the Fraunhofer structures in the solar spectrum.

## 5. GAS CELL AND ZENITH SKY MEASUREMENTS

During the calibration period of the OMI instrument dedicated gas cell measurements and zenith sky measurements were performed with the instrument at flight-representative thermal vacuum temperature and pressure environmental conditions. The gas cell measurements served to validate the above described approach to use the convolution of accurately calibrated slitfunctions with high-resolution literature cross-section spectra in the level 2 data retrieval. The goal of the zenith sky measurements with the OMI instrument was to check its stability and, connected to that, to show its ability to retrieve  $\text{NO}_2$  column densities from atmospheric spectra. These measurements were part of the so-called PI measurement program, and as such performed by scientists of the PI team.

The zenith sky measurements were performed in Delft, The Netherlands, on August 16<sup>th</sup> and 17<sup>th</sup> 2002. The telescope of the instrument was, via two external folding mirrors, pointing towards the zenith, collecting the sunlight scattered from the air column above it. Special care was taken to make the zenith sky beam fill the complete field of view of the telescope in the flight direction, this ensures full and homogeneous illumination of the spectrograph entrance slit so that the features in the spectrum are properly imaged on the detector (inhomogeneous illumination of the width of the spectrograph slit would result in a distortion of the slitfunction).

The weather conditions on both days were warm and sunny with a predominantly bright sky, typical for a nice Dutch summer day. The measurements started before sunrise and lasted until after sunset, covering solar zenith angles between 36 and 95 degrees. Analysis of the individual measurements showed that shift and stretch of the spectrum was very small throughout the day (less than 0.005 pixel over the complete wavelength range), which is an encouraging result regarding the spectral stability of the OMI instrument. Furthermore the data were analyzed for  $\text{NO}_2$  and Ozone. All spectra were ratioed with respect to the measurement taken at solar noon, for which the optical path length through the atmosphere (air-mass factor) prior to being scattered into the instrument is the smallest.

Rayleigh scattering (4th order polynomial) and ring effect were removed from the ratioed spectra. The remaining structures in the resulting residual spectra are attributed to absorption by atmospheric trace gases and show up because of the larger air-mass factor for these measurements. After removal of the fitted trace gas spectrum no systematic features (e.g. a wavelike structure) that could indicate a problem or instability in the data were visible.

Performing a DOAS fit on the spectrum yields a relative slant column density (relative to the noon measurement) for the measurement. Figure 6 shows the relative  $\text{NO}_2$  slant column density that was retrieved from the zenith sky data for August 17th as a function of the solar zenith angle -a Langley plot. The DOAS retrieval was performed on data from the UV2 and from the VIS channel, using 345-373nm and 403-432 nm fit windows respectively. The reference  $\text{NO}_2$  spectrum smeared to OMI resolution was taken from the gas cell measurements. The curves in the Langley plot are smooth, which is a good sign, and the relative slant column densities rapidly increase for large solar zenith angles, which is in accordance with the rapidly increasing air-mass factors for these geometries. The AM curve is lower than the PM curve which agrees with the diurnal variation of  $\text{NO}_2$  in the stratosphere: due to formation of  $\text{N}_2\text{O}_5$  at night and its subsequent, temperature dependent, photodissociation during the day column  $\text{NO}_2$  is expected to be less in the morning than in the afternoon. There is very good compliance between the results obtained from the UV2 and from the VIS channel. Based on these results we are confident that the OMI instrument will be able to retrieve atmospheric  $\text{NO}_2$  column densities from space.

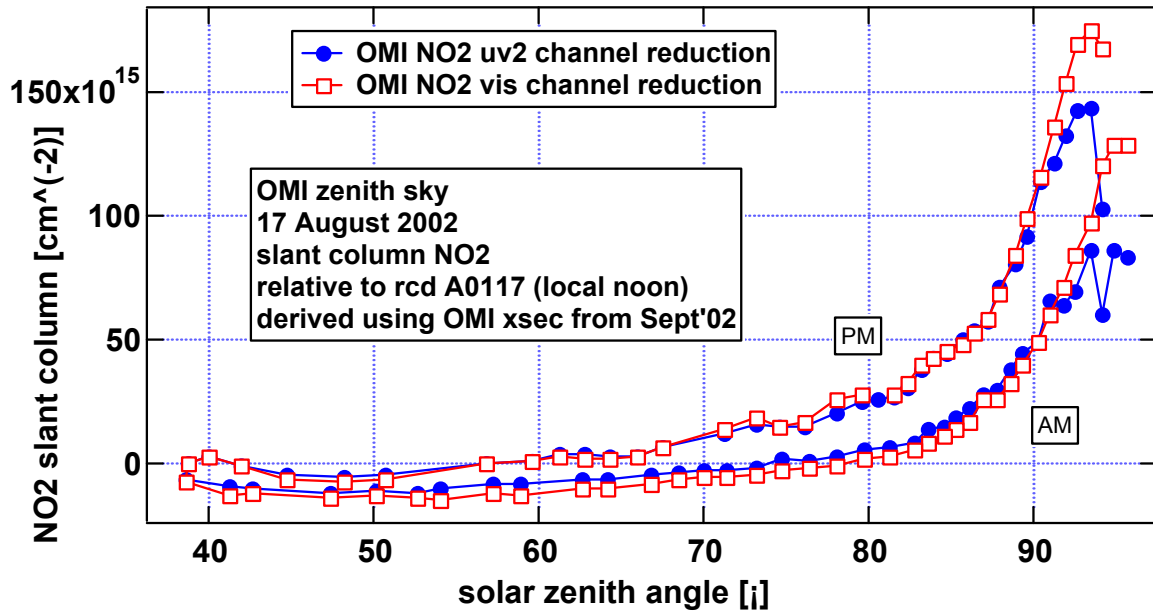


Figure 6: Langley plot of the NO<sub>2</sub> slant column densities relative to local noon versus solar zenith angle, derived from the 17 August 2002 zenith sky measurements with the OMI instrument. The slant columns retrieved from the UV2 and the VIS spectral channel agree very well.

During the gas cell measurement a collimated beam of white light was passed through a 50.0 cm long quartz gas cell and coupled into the instrument via the previously discussed calibration port. The gas cell was continuously flushed with premixed 190ppmv NO<sub>2</sub> in dry air from a gas bottle. The measurements were done with the gas cell at ambient temperature and pressure, meaning that the room-temperature absorption spectrum was measured with the OMI instrument residing at stable thermal vacuum conditions. Measurements were performed with a NO<sub>2</sub> flushed cell and with an empty cell, in the ratio of flushed/empty cell measurements all instrument and light source effects cancel resulting in a residual spectrum solely containing the NO<sub>2</sub> absorption spectrum as seen by the OMI instrument. This OMI recorded NO<sub>2</sub> absorption spectrum is plotted in the upper panel of figure 7 together with a high-resolution NO<sub>2</sub> cross-section spectrum convolved with the calibrated OMI spectral slitfunction. The ratio of both curves, plotted in the lower panel of figure 7, shows the differences between the nearly overlapping curves in the upper plot that are indiscernible by the eye. As seen from the lower plot, the relative difference between the directly measured NO<sub>2</sub> absorption cross-section and the slitfunction convolved literature absorption cross-section is less than 0.2%. This small error proves that the approach followed in the OMI project to use well-calibrated slitfunctions together with high-resolution literature absorption cross-section spectra in the DOAS retrieval of trace gases will work. The residuals in the lower plot of figure 7 exhibit structures that correlate to structures in the NO<sub>2</sub> absorption spectrum, these residual structures most likely arise from imperfections in the slitfunction parameterization and will decrease by refining the parameterization of the slitfunction.

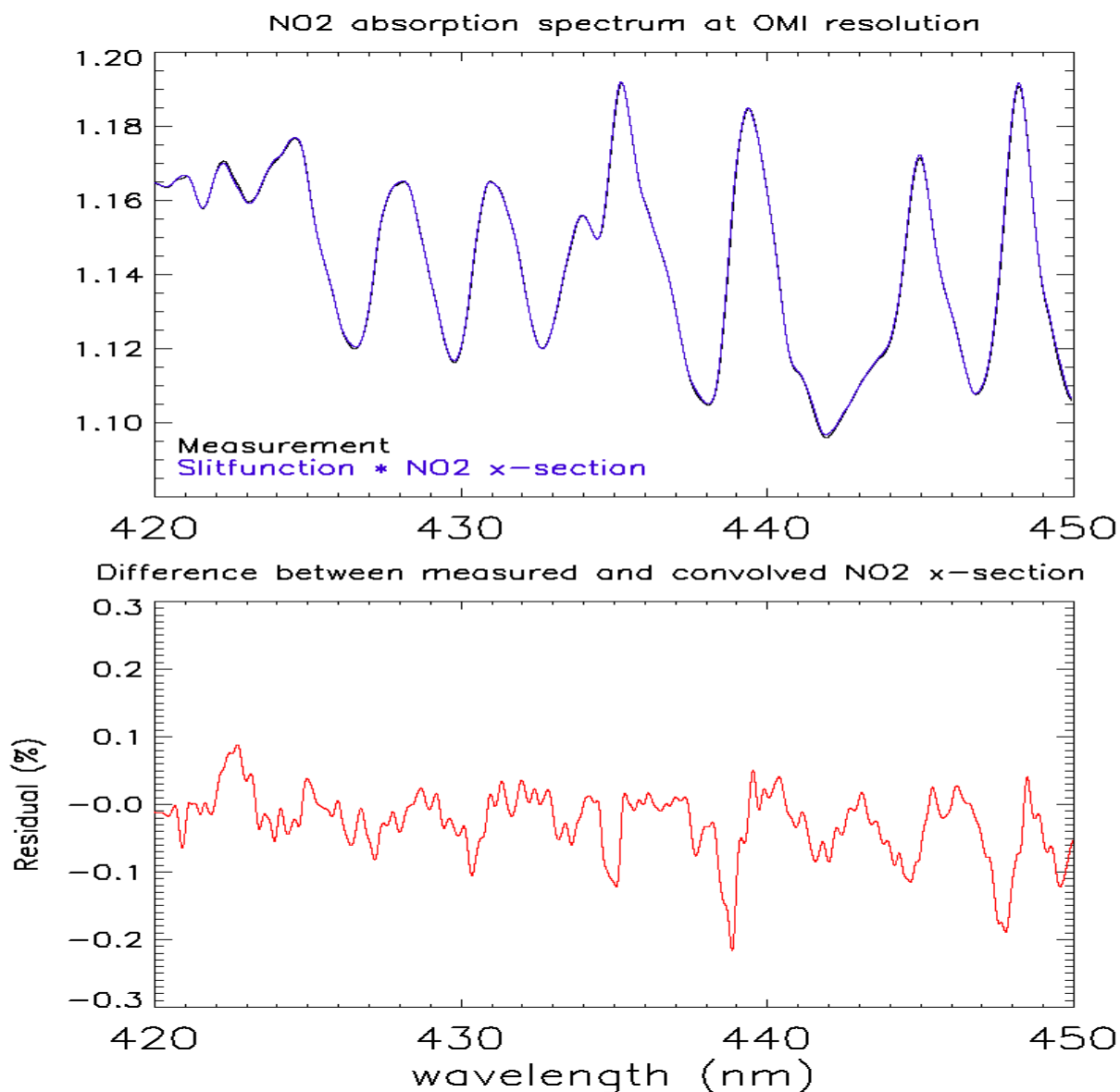


Figure 7: Comparison between the NO<sub>2</sub> absorption cross-section spectrum measured with the OMI instrument and the convolution of a high-resolution literature cross-section spectrum convolved with the calibrated OMI spectral slitfunction. The upper panel shows the co-plotted results, the lower panel shows the difference between both curves. The residuals are smaller than 0.2%, showing that the approach of using accurately calibrated slitfunctions in the data retrieval will work very well.

## 6. CONCLUSIONS

Based on preliminary results of the still ongoing analysis of the calibration measurements of the OMI instrument it can be concluded that regarding the radiometric calibration -absolute (ir)radiance and BSDF- of the instrument certain issues have been identified: the accuracy and of the viewing angle dependency of the absolute (ir)radiance calibration as well as on-board diffuser related features affecting the irradiance and the instrument BSDF. Part of these need to be resolved by using in-flight calibration measurements. A new method was used to accurately calibrate the spectral slitfunction, a high-resolution literature NO<sub>2</sub> absorption cross-section spectrum convolved with the slitfunction agrees very well with the NO<sub>2</sub> gas cell measurements performed with the OMI instrument. The very nice results of the zenith sky measurements inspire confidence that the OMI instrument will be able to measure and retrieve NO<sub>2</sub> column densities from space.